Journal of Computational Physics **178,** 37–57 (2002)
doi:10.1006/jcph.2002.7016, available online at http://www.idealibrary.com on IDEAL®

The Random Projection Method for Stiff Multispecies Detonation Capturing

Weizhu Bao*,[1] and Shi Jin†,[2]

*Department of Computational Science, National University of Singapore, Singapore 117543; and †Department of Mathematics, University of Wisconsin—Madison, Madison, Wisconsin 53706
E-mail: bao@cz3.nus.edu.sg and jin@math.wisc.edu

Received June 9, 2000; revised December 7, 2001

In this paper we extend the random projection method, proposed for general hyperbolic systems with stiff reaction terms, for underresolved numerical simulation of stiff, inviscid, multispecies detonation waves. The key idea in this method is to randomize the ignition temperatures in suitable domains. Several numerical experiments, in both one and two dimensions, demonstrate the reliability and robustness of this novel method.

NOMENCLATURE

B_k	a constant in the frequency factor for the kth reaction
e	total energy
L	the number of different kinds of atoms in all species
M	the number of reactions
N	the number of species
p	pressure
q_m	the heat of formation for the mth species
T	temperature
T_k	ignition temperature for the kth reaction
u	x-component velocity
v	y-component velocity
w_m	mth species source term
W_m	molecular weight of the mth species
z_m	mass fraction of the mth species
α_k	exponent of the temperature dependence of the frequency factor for the kth reaction

[1] Fax: 65-774-6756.

[2] Research supported in part by NSF Grant DMS-0196106.

0021-9991/02 $35.00

γ C_p to C_v ratio
μ_{mn} the number of the nth atom in a molecule of the mth species
ν'_{mk} stoichiometric coefficient for the mth species appearing as a reactant in the kth reaction
ν''_{mk} stoichiometric coefficient for the mth species appearing as a product in the kth reaction
ρ density

1. INTRODUCTION

Consider the reactive Euler equations that model the time-dependent flow of inviscid, compressible, multispecies reacting flows [14, 26],

$$U_t + F(U)_x + G(U)_y = S(U), \tag{1.1}$$

where

$$U = \begin{pmatrix} \rho \\ \rho u \\ \rho v \\ e \\ \rho z_1 \\ \rho z_2 \\ \cdots \\ \rho z_N \end{pmatrix}, \quad F(U) = \begin{pmatrix} \rho u \\ \rho u^2 + p \\ \rho uv \\ (e+p)u \\ \rho u z_1 \\ \rho u z_2 \\ \cdots \\ \rho u z_N \end{pmatrix}, \quad G(U) = \begin{pmatrix} \rho v \\ \rho uv \\ \rho v^2 + p \\ (e+p)v \\ \rho v z_1 \\ \rho v z_2 \\ \cdots \\ \rho v z_N \end{pmatrix}, \quad S(U) = \begin{pmatrix} 0 \\ 0 \\ 0 \\ 0 \\ w_1 \\ w_2 \\ \cdots \\ w_N \end{pmatrix}, \tag{1.2}$$

with

$$w_m = W_m \sum_{k=1}^{M} (\nu''_{mk} - \nu'_{mk}) B_k T^{\alpha_k} e^{-T_k/T} \prod_{j=1}^{N} \left(\frac{\rho z_j}{W_j} \right)^{\nu'_{jk}}, \quad 1 \le m \le N, \tag{1.3}$$

and

$$\sum_{m=1}^{N} z_m = 1. \tag{1.4}$$

The pressure for an ideal gas is given by

$$p = (\gamma - 1)\left(e - \frac{1}{2}\rho(u^2 + v^2) - q_1 \rho z_1 - q_2 \rho z_2 - \cdots - q_N \rho z_N \right), \tag{1.5}$$

and the temperature is defined as $T = p/\rho$.

Equations (1.1)–(1.4) are referred to as the multispecies reactive Euler equations with Arrhenius kinetics. We also consider (1.1)–(1.3) with

$$B_k T^{\alpha_k} e^{-T_k/T}$$

replaced by the Heaviside kinetics

$$B_k T^{\alpha_k} H(T - T_k),$$

where $H(x) = 1$ for $x > 0$ and $H(x) = 0$ for $x < 0$.

One of the main numerical challenges for chemically reacting flows is that the kinetics equations (1.1) often include reactions with widely varying time scales. The chemical time scales, as characterized by B_k^{-1}, may be orders of magnitude faster than the fluid dynamic time scale. This leads to severe problems of numerical stiffness. Even a stable numerical scheme may lead to spurious unphysical solutions unless the small chemical scales are fully resolved numerically.

Developing robust numerical methods for stiff reacting flows has been a very active area of research in the past two decades. In particular, many works have contributed to the analysis and development of *underresolved* numerical methods which are capable of capturing the physically relevant solutions without resolving the small reaction scales. Of course, when one does not resolve the chemical scale numerically (using a grid size larger than the width of the reaction zone), it is impossible to capture the detailed structure (such as the pressure spike) of the reaction zone. Thus the best one can hope is to capture the speed of the discontinuity as well as other features of the fluid dynamics. In the two-species case, i.e., the reaction of type $A \to B$, it was first observed by Colella *et al*. [10] that an underresolved numerical method leads to a spurious weak detonation wave that travels with an incorrect speed. It is known that the smeared numerical shock profile, which exists for all shock-capturing methods, leads to a too-early chemical reaction once the smeared value of the temperature in the numerical shock layer is above the ignition temperature [10, 20]. Since then, lots of attention has been paid to this peculiar numerical phenomenon (see [4, 5, 16, 20, 23]) for the two-species case, and several remedies are available in the literature, for example [3, 11, 18].

Recently we proposed the random projection method as a general and systematic method of solving hyperbolic systems with stiff reaction terms, applicable to reacting flow problems with two species [1]. The origin of a random method can be traced back to the classical work of Glimm [15], and later Chorin successfully adopted it—calling it the random choice method—for reacting flow computation [8]. However, this classical method is a Godunov-type method relying on the solution of the Riemann problem. When applying it to reacting flows one needs to obtain the solution of the generalized Riemann problem for hyperbolic systems with source terms [4]. The random projection method we proposed is a fractional-step method that combines a standard—no Riemann or generalized Riemann solver is needed—shock-capturing method for the homogeneous convection with a strikingly simple random projection step for the reaction term. In the random projection step, the ignition temperature is chosen to be a uniformly distributed random variable between two stable equilibria. When the random sequence is chosen to be the equidistributed van der Corput's sampling sequence [17], we proved, for a model scalar problem, the first-order accuracy on the shock speed if a monotonicity-preserving method—which includes all total variation diminishing (TVD) schemes—is used in the convection step [1]. A large number of numerical experiments for one- and two-dimensional detonation waves demonstrate the robustness of this novel approach for two-species reactions [1, 2].

This novel approach differs from several other numerical methods for front or flame propagation. This is a capturing method that does not reply on the solution of the Riemann problem, as in the front-tracking method [7]. Compared to the level-set methods (e.g., [12, 22, 24]) we use the mass fraction of each species as the natural choice for the level-set function and advance the front with random projection. The drawback of a random method is its statistical fluctuation, which clearly depends on the choice of the random sequences. When we choose the van der Corput sequence, as in a standard Glimm scheme [9], such

a fluctuation is at an acceptable level, as shown in our previous numerical experiments in [1, 2].

In engineering applications, chemically reacting flows often involve more than two species. Sometimes there are tens to hundreds of species [27, 28]. Usually implicit or semiimplicit methods are used in applications where one also considers the viscosity terms (see [6, 13, 21] and references therein for details about resolved calculations). For inviscid flows, underresolved numerical calculation also leads to a spurious nonphysical wave, as shown by one of the numerical examples in Section 5.

In this paper, we extend the random projection method to stiff multispecies reacting flows in both one and two space dimensions. In particular, extensive numerical experiments are conducted to examine the effectiveness and robustness of this novel method. Since the aim is to develop an underresolved numerical method which completely ignores the details of the reaction zone but captures all the main features of the solution outside the reaction zone, it is adequate to formulate this method using the reacting flow model of instantaneous reaction (with a zone-width reaction zone, the so-called Chapman–Jouguet model), in which the chemical heat is released instantaneously. The one-species equations are given, for example, in [8], while the multispecies version is given in Section 3. Formally, when the reaction time goes to zero, Eqs. (1.1)–(1.3) with Arrhenius or Heaviside kinetics reduce effectively to the instantaneous reaction model. Although the rigorous mathematical justification of the "zero reaction limit" is a challenging open issue, the numerical comparisons between the random projection method based on this model with the resolved calculations based on the original kinetics of Arrhenius or Heaviside, as carried out later in this paper, do support the validity of this reduction unless one wants the full details of the reaction layer.

There are certainly restrictions on the instantaneous reaction model or, more generally, on any underresolved numerical method. First, if one needs the details of the reaction layer, then one needs to numerically resolve the layer by solving the full equations (1.1)–(1.3) using fine meshes. Second, these methods cannot predict the instability in overdrive detonation waves since ignoring the reaction layer means that the peak value of pressure, which oscillates due to the instability, cannot be accurately computed. In order to obtain such fine structures one has no choice but to use fine meshes, at least around the reaction zone, by using techniques such as the adaptive mesh refinements.

The paper is organized as follows. In Section 2 we briefly review the random projection method, for a scalar model problem, proposed by the authors [1]. In Section 3 we introduce the random project method for the multispecies problem (1.1) in one space dimension. In Section 4 this method is extended to two space dimensions. In Section 5 several numerical examples, in both one and two space dimensions, are presented. We end in Section 6 with some concluding remarks.

2. REVIEW OF THE RANDOM PROJECTION METHOD FOR A SCALAR MODEL PROBLEM

In this section we review the random projection method, introduced in [1], for the hyperbolic conservation law with stiff reaction term

$$u_t + f(u)_x = -\frac{1}{\varepsilon}(u-\alpha)(u^2-1), \quad -1 < \alpha < 1, \tag{2.1}$$

with piecewise constant initial data

$$u(x,0) = u_0(x) = \begin{cases} 1, & x \le x_0, \\ -1, & x > x_0. \end{cases} \tag{2.2}$$

Here ε is the reaction time, f is a convex function of u, i.e., $f''(u) > 0$, and x_0 is a given point.

The source term in (2.1) admits three local equilibria, i.e., the unstable one, $u = \alpha$, and the stable ones, $u = \pm 1$. When the solution is at equilibria, the reaction term has no effect. Thus the exact solution is a shock discontinuity connecting $u = 1$ with $u = -1$ and propagating to the right with the speed determined by the Rankine–Hugoniot jump condition [20]

$$s = \frac{1}{2}[f(1) - f(-1)]. \tag{2.3}$$

Namely,

$$u(x,t) = \begin{cases} 1, & \text{if } x \le x_0 + st, \\ -1, & \text{if } x > x_0 + st. \end{cases} \tag{2.4}$$

Let h be the spatial increment and k be the time step, such that x_0 is a grid point; i.e., $x_0 = l(0)h$ with $l(0)$ an integer. The numerical solution is evaluated at the points (jh, nk), $j = 0, \pm 1, \pm 2, \ldots, n = 0, 1, 2, \ldots$. Let u_j^n approximate $u(jh, nk)$ and u^n be the solution vector of $u(\cdot, nk)$ at time $t = t_n = nk$. When the reaction term is resolved, i.e., $k = O(h) \ll \varepsilon$, any method which works well for the homogeneous hyperbolic conservation law still works well here. Here we are interested in the underresolved case, where $k = O(h) \gg \varepsilon$.

The random projection method is a fractional step method that solves the homogeneous equation

$$u_t + f(u)_x = 0 \tag{2.5}$$

by a standard shock-capturing method S_c for one time step, followed by a projection step. In the projection step, we replace the unstable equilibrium, or the critical value, α, with a uniformly distributed random sequence $\theta_n \in (-1, 1)$. Let $u^* = S_c(k)u^n$. We define the *random projection* operator $S_\theta(k)$ by

$$S_\theta(k): \quad u_j^{n+1} = \begin{cases} 1, & \text{if } u_j^* > \theta_n, \\ -1, & \text{if } u_j^* \le \theta_n, \end{cases} \quad \text{for all } j. \tag{2.6}$$

In this method, one random value of θ_n will be selected per time step. The combination of the two steps gives the numerical scheme

$$S_{gp}(k): \quad u^{n+1} = S_\theta(k) S_c(k) u^n. \tag{2.7}$$

The stability condition for this method is the usual CFL condition determined by the convection term.

Here and in our practical computations, we always use van der Corput's sampling sequence for $\{\theta_n\}$. The merit of this sequence is that it produces an equidistributed sequence

on the interval [0, 1], and among all known uniformly distributed sequences its deviation is minimal [17]. Let $1 \le n \sum_{k=0}^{m} i_k 2^k$, $i_k = 0, 1$, be the binary expansion of the integer n. Then the van der Corput sequence is defined on [0, 1] as

$$\vartheta_n = \sum_{k=0}^{m} i_k 2^{-(k+1)}, \quad n = 1, 2, \ldots. \tag{2.8}$$

We rescale it in order to get a random number generator θ_n on $[-1, 1]$:

$$\theta_n = 2\vartheta_n - 1, \quad n = 1, 2, \ldots. \tag{2.9}$$

The sequence $\{\theta_n, n = 1, 2, \ldots\}$ is equidistributed on the interval $[-1, 1]$.

We have proved [1] that the random projection method (2.7), in which a monotonicity-preserving method S_c—which includes all TVD methods—is used for the convection term, can capture the correct location of discontinuities for the scalar model problem (2.1), (2.2) with first-order accuracy. Let $l(n) - l(0)$ be the number of grid points that the discontinuity has traveled after n time steps.

THEOREM 2.1 [1]. *Given $T > 0$, let S_c be a monotonicity-preserving method. The difference between the shock location of the exact solution, $x_0 + st_n$, and the numerical one, $l(n)h$, as determined by the random projection method* (2.7), *has the estimate*

$$|x_0 + st_n - l(n)h| \le C(T)h|\ln h|, \tag{2.10}$$

for any $0 < t_n \le T$, and fixed $\lambda = sk/h$, where $C(T)$ is a positive constant depending on $|\ln(T)|$.

This shows that the shock location is captured with first-order accuracy for all time, although the reaction time ε is not resolved numerically. In [1, 2], this method was generalized to two-species stiff detonation wave computation, where the key idea is to randomize the ignition temperature in a suitable domain. In the following two sections, we extend the random projection method to one- and two-dimensional multispecies detonation computation. Although the theorem was proved only for the scalar case, we observe numerically first-order convergence for systems, as is reported in Section 5.

3. ONE SPACE DIMENSION

In this section, we describe the random projection method for the stiff multispecies reacting flows in one space dimension. We use $U_j^n = (\rho_j^n, (\rho u)_j^n, e_j^n, (\rho z_1)_j^n, (\rho z_2)_j^n, \ldots, (\rho z_N)_j^n)^T$ to denote the approximate solution of $U = (\rho, \rho u, e, \rho z_1, \rho z_2, \ldots, \rho z_N)^T$ at the point (x_j, t_n). Our main interest is an underresolved numerical method which allows $k = O(h) \gg (1/B_k)$, yet still obtains physically relevant numerical solutions.

Consider the Riemann initial data

$$\begin{aligned}&(\rho(x,0), u(x,0), p(x,0), z_1(x,0), z_2(x,0), \ldots, z_N(x,0))\\ &\quad = \begin{cases} (\rho_l(x), u_l(x), p_l(x), (z_1)_l, (z_2)_l, \ldots, (z_N)_l), & \text{if } x \le x_0,\\ (\rho_r(x), u_r(x), p_r(x), (z_1)_r, (z_2)_r, \ldots, (z_N)_r), & \text{if } x > x_0, \end{cases}\end{aligned} \tag{3.1}$$

where x_0 is a given point and $\sum_{m=1}^{N}(z_m)_l = \sum_{m=1}^{N}(z_m)_r = 1$. In addition the initial mass fraction should satisfy the following condition:

$$\sum_{m=1}^{N} \frac{\mu_{mn}(z_m)_l}{W_m} = \sum_{m=1}^{N} \frac{\mu_{mn}(z_m)_r}{W_m}, \quad 1 \le n \le L. \tag{3.2}$$

The above equalities guarantee the conservation of the number of atoms in the reactions. We also assume that after the reaction, at least one species disappears (fully reacted). Thus there exists a j such that $(z_j)_l = 0$ for each reaction. This implies that

$$(w_m)_l = 0, \quad \text{for all } m = 1, 2, \ldots, N. \tag{3.3}$$

This assumption clearly holds outside the reaction zone. Since an underresolved method ignores the reaction zone of width $O(\frac{1}{B_k})$, each species has only two physical states, either $(z_m)_l$ or $(z_m)_r$. Without loss of generality the data in (3.1) are chosen such that the discontinuity, initially at $x = x_0$, moves to the right. The case when the discontinuity moves to the left can be treated similarly.

The random projection method is a fractional-step method,

$$S_1(k): \quad U^{n+1} = S_p(k) S_F(k) U^n, \tag{3.4}$$

that consists of solving the homogeneous convection

$$U_t + F(U)_x = 0 \tag{3.5}$$

by a standard shock-capturing method, denoted by $S_F(k)$, for one time step, followed by a random projection step for the stiff chemical reaction terms

$$\rho_t = 0, \quad (\rho u)_t = 0, \quad e_t = 0, \quad (\rho z_1)_t = w_1, \quad (\rho z_2)_t = w_2, \ldots, \quad (\rho z_N)_t = w_N. \tag{3.6}$$

Due to (3.3), the above ODE collapses to a simple projection,

$$(z_m)_j^{n+1} = \begin{cases} (z_m)_l, & \text{if } T_j^* \le \min_k T_k, \\ (z_m)_r, & \text{if } T_j^* > \max_k T_k, \end{cases} \quad \text{for all } j, \tag{3.7}$$

with $U^* = S_F(k)U^n$, $T_j^* = p_j^*/\rho_j^*$ being the values after the convection step. However, on the discrete spatial domain, due to the grid effect, this projection (referred to as the deterministic projection) yields an incorrect speed, since the smeared value of the temperature T^* in the detonation layer, once above $\max_k T_k$, will trigger the chemical reaction too early. The key idea in the random projection method is to use a randomized ignition temperature in a suitable domain. This strategy could be successful since the speed of the front does not depend on the specific value of T_k, as long as it is in the range between the equilibrium states T_l and T_r on both sides of the detonation. We now describe the details of this random projection step.

Let

$$\theta_n = (T_l - T_r)\vartheta_n + T_r, \quad T_l = \min_{x<x_0} \frac{p_l(x,0)}{\rho_l(x,0)}, \quad T_r = \max_{x>x_0} \frac{p_r(x,0)}{\rho_r(x,0)}, \tag{3.8}$$

where ϑ_n is the van der Corput's sequence [see (2.8) for detail]. Thus θ_n is an equidistributed sequence over the domain $[T_l, T_r]$. Assume $x_0 = l(0)h$ is a grid point. The projection always makes z_m either $(z_m)_l$ or $(z_m)_r$ for all $1 \le m \le N$; therefore at any time step t_n, there is an $l(n) = j_0$, with j_0 being an integer, such that

$$(z_m)_j^n = \begin{cases} (z_m)_l, & \text{if } j \le l(n), \\ (z_m)_r, & \text{if } j > l(n), \end{cases} \quad 1 \le m \le N. \tag{3.9}$$

Here $l(n)$ is the location of the jump for z_m^n. The random projection will be performed around $x = l(n)h$, a procedure referred to as the *local random projection* in [1].

Let d be the estimated number of smeared points in the detonation layer. Modern shock-capturing methods always introduce a few smeared points across the discontinuity. The information on d can easily by obtained from numerical experience (normally between 1 and 5). We now move the jump of z_m according to the following algorithm:

$$\begin{aligned} S_p(k)\colon\quad & \rho^{n+1} = \rho^*, \quad m^{n+1} = m^*, \quad e^{n+1} = e^*; \\ & \text{set } l(n+1) := l(n) - 1; \\ & \text{For } l = l(n) - 1, \ldots, l(n) + d, \text{ do} \\ & \quad l(n+1) := l, \quad \text{if } T_l^* > \theta_n; \\ & (z_m)_j^{n+1} = \begin{cases} (z_m)_l, & \text{if } j \le l(n+1), \\ (z_m)_r, & \text{if } j > l(n+1), \end{cases} \quad \text{for all } m,\ j. \end{aligned} \tag{3.10}$$

In the above algorithm, only $d + 2$ points will be scanned. The stability condition for the algorithm (3.4) is the usual CFL condition determined from the convection step $S_F(k)$.

For numerical comparison, we also use the *deterministic method*, which discretizes the chemical reaction term (3.6), with T_k fixed as given by the original problem, by an implicit method (for example, the backward Euler method) and solving the corresponding nonlinear system using Newton's method.

4. TWO SPACE DIMENSIONS

In this section, the random projection method is extended to two-dimensional multispecies reacting flows (1.1). For simplicity, we consider the flow in a two-dimensional channel. Let the initial data be

$$\begin{aligned} &(\rho(x, y, 0), u(x, y, 0), v(x, y, 0), p(x, y, 0), z_1(x, y, 0), z_2(x, y, 0), \ldots, z_N(x, y, 0)) \\ &\quad = \begin{cases} (\rho_l, u_l, v_l, p_l, (z_1)_l, (z_2)_l, \ldots, (z_N)_l), & \text{if } x \le \xi(y), \\ (\rho_r, u_r, v_r, p_r, (z_1)_r, (z_2)_r, \ldots, (z_N)_r), & \text{if } x > \xi(y), \end{cases} \end{aligned} \tag{4.1}$$

where $\xi(y)$ is a given function of y. These data are chosen such that the discontinuity moves to the right and with the same assumptions on $(z_m)_l$ and $(z_m)_r$ as in the 1D case. Let

$$\theta_n = (T_l - T_r)\vartheta_n + T_r, \quad T_l = \frac{p_l}{\rho_l}, \quad T_r = \frac{p_r}{\rho_r}, \tag{4.2}$$

with ϑ_n being the van der Corput sampling sequence on the interval [0, 1] defined in (2.8).

Let the grid points $(x_i, y_j) = (ih, jh)$, $i, j = \ldots, -1, 0, 1, \ldots$, with equal mesh spacing h. The time levels $t_n = nk$, $k = 0, 1, 2, \ldots$ are also uniformly spaced with time step k. Let $U_{ij}^n = (\rho_{ij}^n, (\rho u)_{ij}^n, (\rho v)_{ij}^n, e_{ij}^n, (\rho z_1)_{ij}^n, (\rho z_2)_{ij}^n, \ldots, (\rho z_N)_{ij}^n)$ be the approximate solution of $U = (\rho, \rho u, \rho v, e, \rho z_1, \rho z_2, \ldots, \rho z_N)$ at (x_i, y_i, t_n). Similarly to the one-dimensional case, the random projection method is a fractional-step method that consists of a standard shock-capturing method for the homogeneous convection

$$U_t + F(U)_x + G(U)_y = 0, \tag{4.3}$$

denoted by $S_{FG}(k)$ for one step, followed by a random projection step for the stiff chemical reaction terms

$$\begin{gathered} \rho_t = 0, \quad (\rho u)_t = 0, \quad (\rho v)_t = 0, \quad e_t = 0, \quad (\rho z_1)_t = w_1, \\ (\rho z_2)_t = w_2, \ldots, \quad (\rho z_N)_t = w_N, \end{gathered} \tag{4.4}$$

where T_k, the ignition temperatures, are randomized in suitable domains.

Notice that at any time step, for each j there is an $l_j(n) = j_n$, with j_n being an integer, such that

$$(z_m)_{ij}^n = \begin{cases} (z_m)_l, & \text{if } i \le l_j(n), \\ (z_m)_r, & \text{if } i > l_j(n), \end{cases} \quad 1 \le m \le N. \tag{4.5}$$

Here $l_j(n)$ is the location of the jump for the numerical solution of z_m along the line $y = y_j$ at time t_n. Let $U^* = S_{FG}(k)U^n$, and let d be the estimated number of smeared points in the detonation layer. Then the random project algorithm for the chemical reaction term (4.4) is

$$\begin{aligned} S_{2p}(k)\colon\ & \rho^{n+1} = \rho^*, \quad u^{n+1} = u^*, \quad v^{n+1} = v^*, \quad e^{n+1} = e^*; \\ & \text{For } j \text{ do} \\ & \quad \text{Set } l_j(n+1) := l_j(n) - 1, \\ & \quad \text{For } r = l_j(n) - 1, l_j(n), \ldots, l_j(n) + d, \text{ do} \\ & \quad\quad l_j(n+1) := r, \text{ if } T_{rj}^* > \theta_n, \\ & (z_m)_{ij}^{n+1} = \begin{cases} (z_m)_l, & \text{if } i \le l_j(n+1), \\ (z_m)_r, & \text{if } i > l_j(n+1), \end{cases} \quad \text{for all } m, i. \end{aligned} \tag{4.6}$$

The combination of the two steps gives

$$S_2(k)\colon\ U^{n+1} = S_{2p}(k)S_{FG}(k)U^n. \tag{4.7}$$

The stability condition for this algorithm is still the usual CFL condition determined from the convection step $S_{FG}(k)$.

5. NUMERICAL EXAMPLES

In order to verify the performance of the random projection method for stiff multispecies detonation computations, we conducted several numerical experiments in both one and two dimensions. In our computation, the operators $S_F(k)$ and $S_{FG}(k)$ are the second-order

relaxed scheme [19], which is a TVD scheme without the use of Riemann solvers or local characteristic decompositions. We choose $d = 5$ in (3.4) and (4.7) and use the Heaviside kinetics in (1.3) in our computations in this section. It is known that the stiffness problem is more severe in the Heaviside case than in the Arrhenius case [11].

In these tests, the hydrodynamic data (such as pressure, mass, velocity) are chosen artificially rather than from physical experiments.

EXAMPLE 5.1. We consider a reacting model

$$2A + B \to 2C.$$

A prototype reaction for this model is

$$2H_2 + O_2 \to 2H_2O.$$

In this problem, there are three species and one reaction. The parameters are $M = 1$, $N = 3$, $\gamma = 1.4$, $T_1 = 2.0$, $B_1 = 10^6$, $\alpha_1 = 0$, $q_1 = 100$, $q_2 = 0.0$, $q_3 = 0.0$, $W_1 = 2$, $W_2 = 32$, $W_3 = 18$, $\nu'_{1,1} = 2$, $\nu'_{2,1} = 1$, $\nu'_{3,1} = 0$, $\nu''_{1,1} = 0$, $\nu''_{2,1} = 0$, and $\nu''_{3,1} = 2$. The initial data are piecewise constants given by

$$(\rho, u, p, z_1, z_2, z_3)(x, 0) = \begin{cases} (\rho_l, u_l, p_l, (z_1)_l, (z_2)_l, (z_3)_l), & \text{if } x \le 2.5, \\ (\rho_r, u_r, p_r, (z_1)_r, (z_2)_r, (z_3)_r), & \text{if } x > 2.5, \end{cases}$$

where $p_l = 20.0$, $\rho_l = 2.0$, $u_l = 8.0$, $(z_1)_l = 0.0$, $(z_2)_l = 0.0$, and $(z_3)_l = 1.0$, and where $p_r = 1.0$, $\rho_r = 1.0$, $u_r = 0$, $(z_1)_r = \frac{1}{9}$, $(z_2)_l = \frac{8}{9}$, and $(z_3)_r = 0.0$. This problem is solved on the interval [0, 50].

The exact solution consists of a detonation wave, followed by a contact discontinuity and a shock, all moving to the right. We obtain the "exact" solution by an explicit method (the second-order relaxed scheme for the convection terms followed by a forward Euler method for the chemical reaction terms) using a fine mesh size $h = 0.0025$ (i.e., 20,001 grid points on the interval [0, 50]) and a small time step $k = 0.0001$ and denote the solution by $(\rho^e, u^e, p^e, z_1^e, z_2^e, z_3^e)$. This is a resolved calculation. We compare the results obtained by the local random projection method (3.4) and the deterministic method using a coarse mesh $h = 0.25$ (i.e., 201 grid points on the interval [0, 50]) and large time step $k = 0.01$, and we output the numerical solutions at $t = 4.0$.

Figure 1a shows the numerical solution by the random projection method (3.4), while Fig. 1b shows the numerical solution by the deterministic method. It can be seen that the random projection method captures the correct speed of the discontinuity even when the reaction scale is not numerically resolved. The shock and the detonation front are captured with a higher resolution than the contact discontinuity, a typical phenomenon for shock-capturing methods. The location of z_m may be few grid points away from the exact location due to random effect, but such a deviation does not grow in time. There are small postshock statistical fluctuations due to the random nature of the method, but they are at an acceptable level. The deterministic method produces spurious nonphysical waves, as was observed in earlier literature for stiff reacting flows with two species.

To do a numerical convergence study of the random project method for stiff multispecies detonation capturing in order to verify $O(h)$ accuracy, let $(\rho^h, u^h, p^h, z_1^h, z_2^h, z_3^h)$ denote the numerical solution of (1.1)–(1.3) with initial condition (3.1) by using our random projection

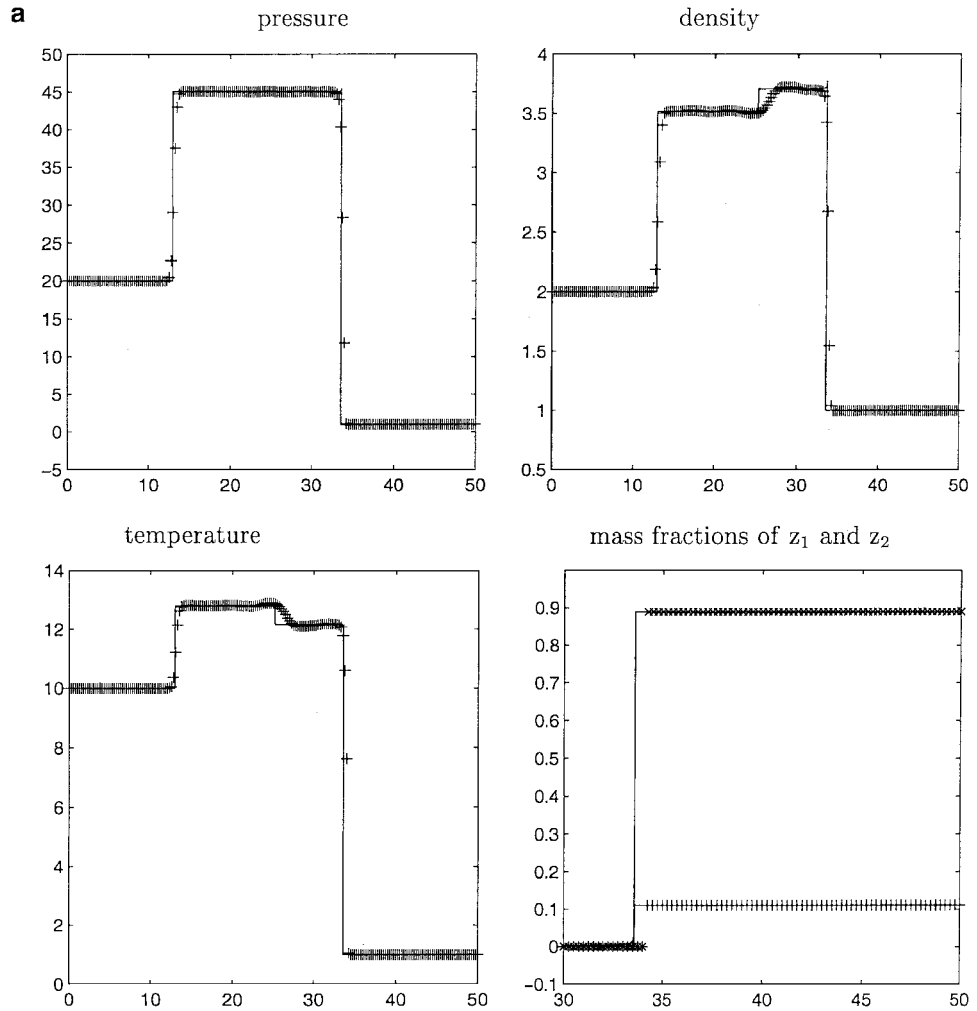

FIG. 1. Numerical solutions of Example 5.1 at $t = 4.0$ calculated with $h = 0.25$, $k = 0.01$. $-$, "Exact" solutions; $++$, computed solutions. In the last graph, $++ = z_1$ and $\text{xx} = z_2$. (a) The random projection method (3.4). (b) The deterministic method.

method under mesh size h and time step $k = 0.002$ and define the mean discrete L^1-norm of a function $f = (f_0, f_1, \ldots, f_N)^T$ on the interval $[a, b]$ by

$$\|f\|_{L^1,h} = \frac{1}{N}\sum_{i=0}^{N} |f_i| = \frac{h}{b-a}\sum_{i=0}^{N} |f_i|.$$

Tables I–III show the mean L^1-error of the numerical solution by using our random projection method for this example at $t = 1.0$, $t = 2.0$, and $t = 4.0$, respectively.

From Tables I–III, we observe numerically first-order convergence of our random projection method applied to stiff multispecies detonation capturing. Furthermore the errors almost do not change with time.

In all of the following examples, the deterministic method always produces spurious nonphysical waves when the reaction scale is not resolved. We do not report those results and only present the solutions obtained by the random projection method.

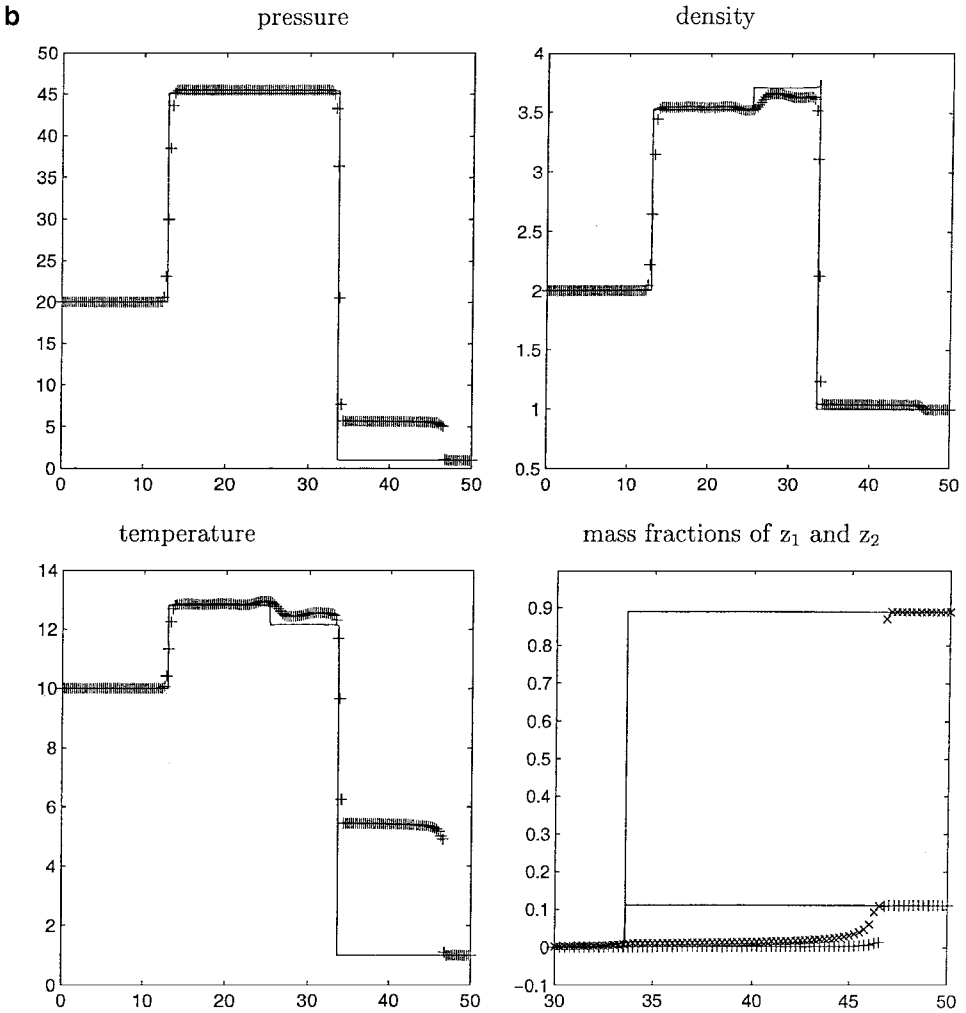

FIG. 1—*Continued*

EXAMPLE 5.2. The setup of this example is similar to that in Example 5.1 except that here $q_1 = 1000$, $B_1 = 500$, $\alpha_1 = 1$, $u_l = 10.0$, $p_l = 40.0$, $(z_1)_l = 0.325$, $(z_2)_l = 0.0$, $(z_3)_l = 0.675$, $(z_1)_r = 0.4$, $(z_2)_r = 0.6$, and $(z_3)_r = 0.0$.

The exact solution consists of a detonation wave, followed by a contact discontinuity and a shock, all moving to the right. We obtain the "exact" solution similarly as that in

TABLE I

Errors of the Numerical Solution by the Random Projection Method at $t = 1.0$

	$h = 0.5$	$h = 0.25$	$h = 0.125$	$h = 0.0625$	$h = 0.025$
$\|u^e - u^h\|_{L^1,h}$	0.958E-1	0.408E-1	0.216E-1	0.117E-1	0.574E-2
$\|p^e - p^h\|_{L^1,h}$	0.7330	0.3349	0.1791	0.940E-1	0.4243E-1
$\|\rho^e - \rho^h\|_{L^1,h}$	0.524E-1	0.258E-1	0.136E-1	0.744E-2	0.346E-2
$\|z_1^e - z_1^h\|_{L^1,h}$	0.225E-2	0.116E-2	0.592E-3	0.310E-3	0.141E-3
$\|z_2^e - z_2^h\|_{L^1,h}$	0.180E-1	0.925E-2	0.473E-2	0.248E-2	0.113E-2

TABLE II
Errors of the Numerical Solution by the Random Projection Method at $t = 2.0$

	$h = 0.5$	$h = 0.25$	$h = 0.125$	$h = 0.0625$	$h = 0.025$
$\|u^e - u^h\|_{L^1,h}$	0.796E-1	0.442E-1	0.231E-1	0.133E-1	0.537E-2
$\|p^e - p^h\|_{L^1,h}$	0.6558	0.3645	0.1848	0.1004	0.391E-2
$\|\rho^e - \rho^h\|_{L^1,h}$	0.502E-1	0.273E-1	0.147E-1	0.800E-2	0.336E-2
$\|z_1^e - z_1^h\|_{L^1,h}$	0.229E-2	0.116E-2	0.601E-3	0.321E-3	0.156E-3
$\|z_2^e - z_2^h\|_{L^1,h}$	0.183E-1	0.929E-2	0.481E-2	0.257E-2	0.125E-2

Example 5.1. Figure 2 shows the numerical solutions by the random projection method (3.4) with $h = 0.25$ (i.e., 201 grid points on the interval [0, 50]) and $k = 0.01$ at time $t = 3.0$. All discontinuities are captured numerically.

EXAMPLE 5.3. We consider a reacting model

$$A + 2B \to C + 2D.$$

A prototype reaction for this model is

$$CH_4 + 2O_2 \to CO_2 + 2H_2O.$$

In this problem, there are four species and one reaction. The parameters are $M = 1$, $N = 4$, $\gamma = 1.4$, $T_1 = 2.0$, $B_1 = 10^6$, $\alpha_1 = 0$, $q_1 = 500$, $q_2 = 0.0$, $q_3 = 0.0$, $q_4 = 0.0$, $W_1 = 16$, $W_2 = 32$, $W_3 = 44$, $W_4 = 18$, $\nu'_{1,1} = 1$, $\nu'_{2,1} = 2$, $\nu'_{3,1} = 0$, $\nu'_{4,1} = 0$, $\nu''_{1,1} = 0$, $\nu''_{2,1} = 0$, $\nu''_{3,1} = 1$, and $\nu''_{4,1} = 2$. The initial data are

$$(\rho, u, p, z_1, z_2, z_3, z_4)(x, 0) = \begin{cases} (\rho_l, u_l, p_l, (z_1)_l, (z_2)_l, (z_3)_l, (z_4)_l), & \text{if } x \le 2.5, \\ (\rho_r, u_r, p_r, (z_1)_r, (z_2)_r, (z_3)_r, (z_4)_r), & \text{if } x > 2.5, \end{cases}$$

where $p_l = 40.0$, $\rho_l = 2.0$, $u_l = 10.0$, $(z_1)_l = 0.0$, $(z_2)_l = 0.2$, $(z_3)_l = 0.475$, and $(z_4)_l = 0.325$, and where $p_r = 1.0$, $\rho_r = 1.0$, $u_r = 0$, $(z_1)_r = 0.1$, $(z_2)_r = 0.6$, $(z_3)_r = 0.2$, and $(z_4)_r = 0.1$.

The exact solution consists of a detonation wave followed by a contact discontinuity and a shock, all moving to the right. We obtain the "exact" solution similarly to that in Example 5.1. Figure 3 shows the numerical solutions by the random projection method (3.4) with $h = 0.25$ (i.e., 201 grid points on the interval [0, 50]) and $k = 0.01$ at time $t = 3.0$. All discontinuities are captured numerically.

TABLE III
Errors of the Numerical Solution by the Random Projection Method at $t = 4.0$

	$h = 0.5$	$h = 0.25$	$h = 0.125$	$h = 0.0625$	$h = 0.025$
$\|u^e - u^h\|_{L^1,h}$	0.863E-1	0.469E-1	0.264E-1	0.114E-1	0.537E-2
$\|p^e - p^h\|_{L^1,h}$	0.7170	0.3777	0.2110	0.867E-1	0.447E-1
$\|\rho^e - \rho^h\|_{L^1,h}$	0.540E-1	0.299E-1	0.158E-1	0.722E-2	0.374E-2
$\|z_1^e - z_1^h\|_{L^1,h}$	0.229E-2	0.118E-2	0.894E-3	0.344E-3	0.185E-3
$\|z_2^e - z_2^h\|_{L^1,h}$	0.184E-1	0.940E-2	0.473E-2	0.275E-2	0.148E-2

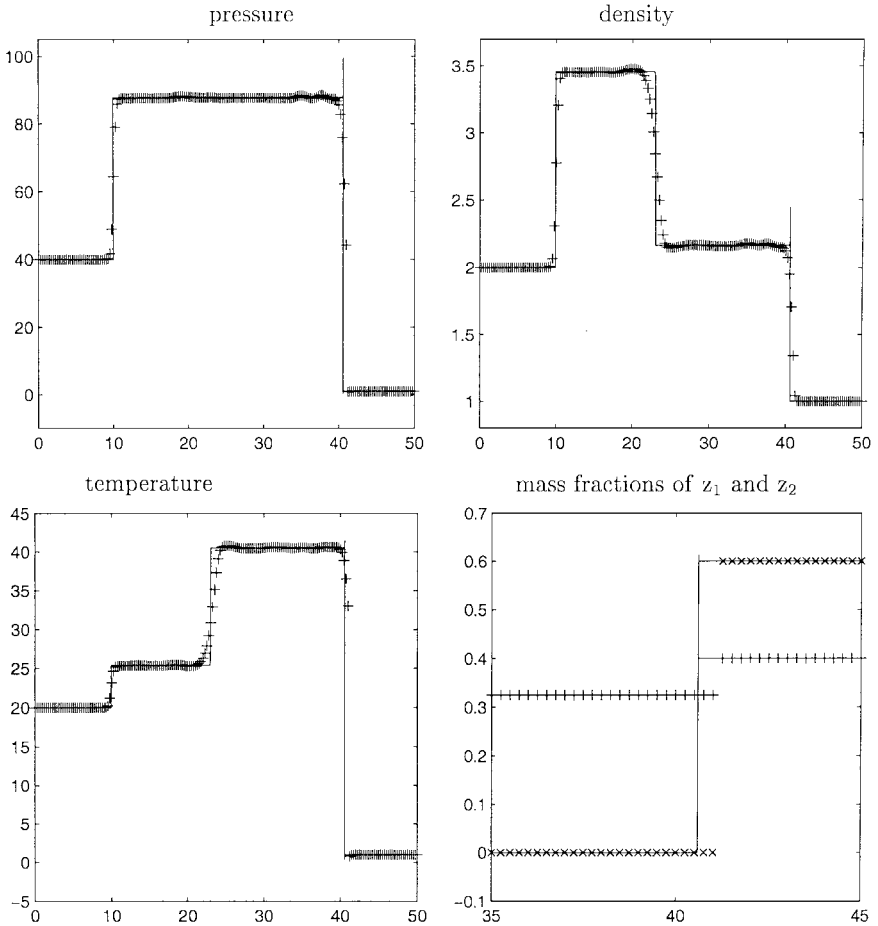

FIG. 2. Numerical solutions of Example 5.2 at $t = 3.0$ calculated by the random projection method (3.4) with $h = 0.25$, $k = 0.01$. $-$, "Exact" solutions; $++$, computed solutions. In the last graph, $++ = z_1$ and $\mathrm{xx} = z_2$.

EXAMPLE 5.4. We consider a reacting model

$$A + B \to 2C, \quad 2C + A \to 2D,$$

with species E appearing as a catalyst. A prototype reaction for this model is

$$H_2 + O_2 \to 2OH, \quad 2OH + H_2 \to 2H_2O,$$

with N_2 appearing as a catalyst. In this problem, there are five species and two reactions. The parameters are $M = 2$, $N = 5$, $\gamma = 1.4$, $T_1 = 2.0$, $T_2 = 10.0$, $B_1 = 10^5$, $B_2 = 2 \times 10^4$, $\alpha_1 = \alpha_2 = 0$, $q_1 = 0.0$, $q_2 = 0.0$, $q_3 = -20.0$, $q_4 = -100.0$, $q_5 = 0.0$, $W_1 = 2$, $W_2 = 32$, $W_3 = 17$, $W_4 = 18$, $W_5 = 28$, $\nu'_{1,1} = 1$, $\nu'_{2,1} = 1$, $\nu'_{3,1} = 0$, $\nu'_{4,1} = 0$, $\nu'_{5,1} = 0$, $\nu'_{1,2} = 1$, $\nu'_{2,2} = 0$, $\nu'_{3,2} = 2$, $\nu'_{4,2} = 0$, $\nu'_{5,2} = 0$, $\nu''_{1,1} = 0$, $\nu''_{2,1} = 0$, $\nu''_{3,1} = 2$, $\nu''_{4,1} = 0$, $\nu''_{5,1} = 0$, $\nu''_{1,2} = 0$, $\nu''_{2,2} = 0$, $\nu''_{3,2} = 0$, $\nu''_{4,2} = 2$, and $\nu''_{5,2} = 0$. The initial data are

$$(\rho, u, p, z_1, z_2, z_3, z_4, z_5)(x, 0) = \begin{cases} (\rho_l, u_l, p_l, (z_1)_l, (z_2)_l, (z_3)_l, (z_4)_l, (z_5)_l), & \text{if } x \le 2.5, \\ (\rho_r, u_r, p_r, (z_1)_r, (z_2)_r, (z_3)_r, (z_4)_r, (z_5)_r), & \text{if } x > 2.5, \end{cases}$$

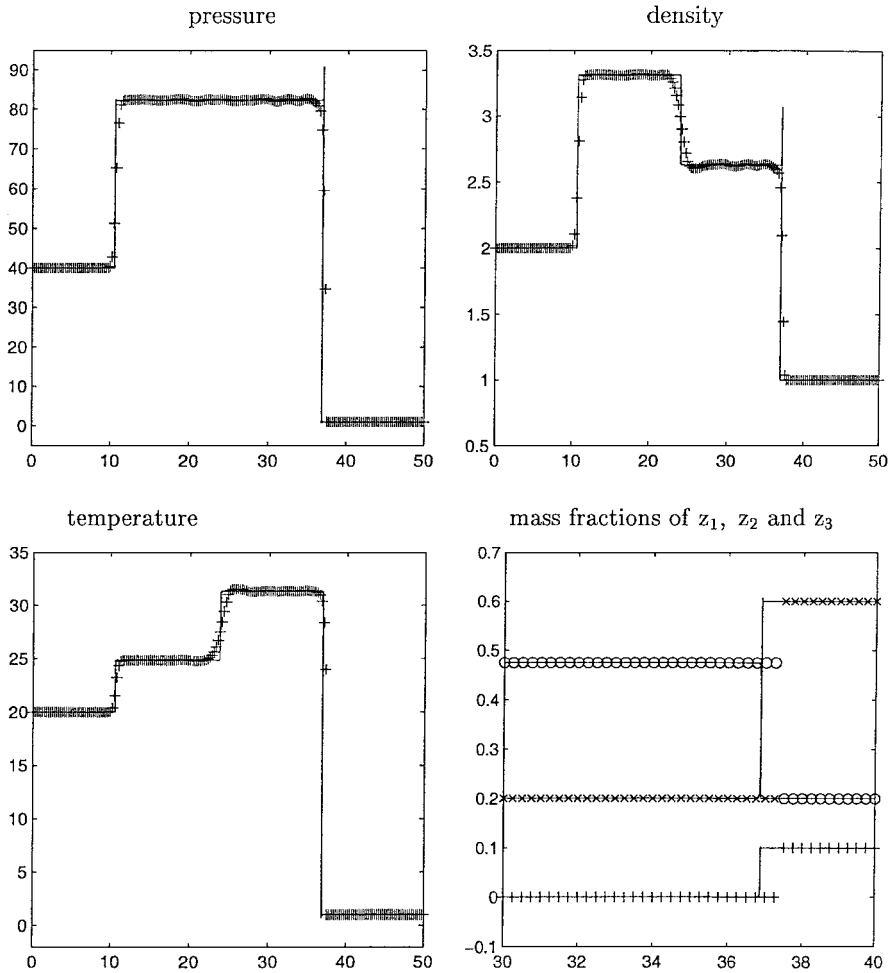

FIG. 3. Numerical solutions of Example 5.3 at $t = 3.0$ calculated by the random projection method (3.4) with $h = 0.25$, $k = 0.01$. $-$, "Exact" solutions; $++$, computed solutions. In the last graph, $++ = z_1$, xx $= z_2$, and oo $= z_3$.

where $p_l = 40.0$, $\rho_l = 2.0$, $u_l = 10.0$, $(z_1)_l = 0.08$, $(z_2)_l = 0.72$, $(z_3)_l = 0.0$, $(z_4)_l = 0.0$, and $(z_5)_l = 0.2$, and where $p_r = 1.0$, $\rho_r = 1.0$, $u_r = 0.0$, $(z_1)_r = 0.0$, $(z_2)_r = 0.0$, $(z_3)_r = 0.17$, $(z_4)_r = 0.63$, and $(z_5)_r = 0.2$.

The exact solution consists of a detonation wave followed by a rarefaction wave and a shock, all moving to the right. We obtain the "exact" solution similarly to that in Example 5.1. Figure 4 shows the numerical solutions by the random projection method (3.4) with $h = 0.25$ (i.e., 201 grid points on the interval [0, 50]) and $k = 0.01$ at time $t = 3.0$. All waves are captured numerically with the correct speeds.

The above examples demonstrate that the random projection method works effectively for one-dimensional stiff multispecies detonations, although the reaction scales are not numerically resolved. It captures the correct speeds of detonations, as well as other standard fluid dynamical structures with high resolutions. The deterministic method, however, always produces spurious waves when the chemical scale is not numerically resolved.

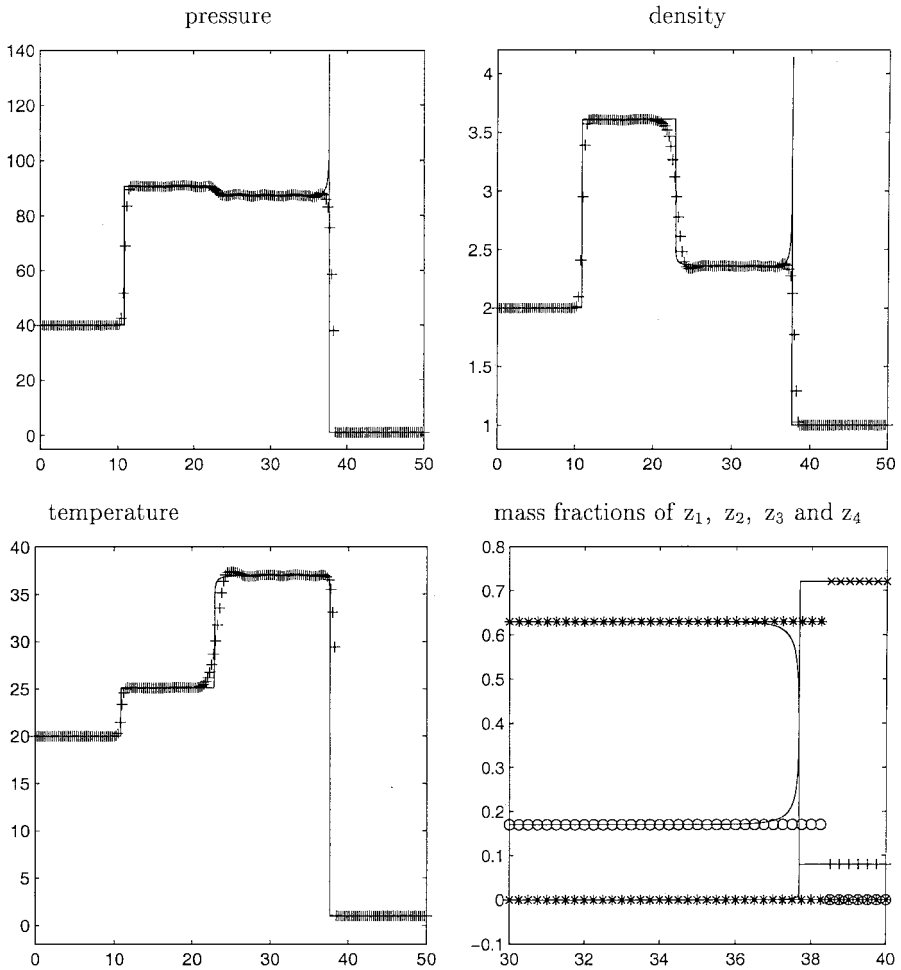

FIG. 4. Numerical solutions of Example 5.4 at $t = 3.0$ calculated by the random projection method (3.4) with $h = 0.25$, $k = 0.01$. $-$, "Exact" solutions; $++$, computed solutions. In the last graph, $++ = z_1$, $\mathrm{xx} = z_2$, $\mathrm{oo} = z_3$, and $** = z_4$.

EXAMPLE 5.5. This is a two-dimensional example with radial symmetry analogous to Example 5.3; i.e., the parameters $M, N, \gamma, T_1, B_1, \alpha_1, q_1, \ldots, \nu''_{4,1}$ are the same as those in Example 5.3 except $q_1 = 100$. A similar example, but with only two species, was used in [18]. The initial values consist of totally burnt gas inside of a circle with radius 10 and totally unburnt gas everywhere outside of the circle. Furthermore the unburnt and burnt states are chosen in a way analogous to the one-dimensional case, i.e.,

$$(\rho, u, v, p, z_1, z_2, z_3, z_4)(x, y, 0) = \begin{cases} (\rho_l, u_l(x, y), v_l(x, y), p_l, (z_1)_l, (z_2)_l, (z_3)_l, (z_4)_l), & \text{if } r \le 10, \\ (\rho_r, u_r, v_r, p_r, (z_1)_r, (z_2)_r, (z_3)_r, (z_4)_r), & \text{if } r > 10, \end{cases}$$

where $r = \sqrt{x^2 + y^2}$, $p_l = 40.0$, $\rho_l = 2.0$, $u_l = 10x/r$, $v_l = 10y/r$, $(z_1)_l = 0.0$, $(z_2)_l = 0.2$, $(z_3)_l = 0.475$, and $(z_4)_l = 0.325$, and where $p_r = 1.0$, $\rho_r = 1.0$, $u_r = 0.0$, $v_r = 0.0$, $(z_1)_r = 0.1$, $(z_2)_r = 0.6$, $(z_3)_r = 0.2$, and $(z_4)_r = 0.1$.

This is a radially symmetric problem and the important feature is that the detonation front is circular. This problem is solved on the domain $[0, 50] \times [0, 50]$ with $h = 0.5$ and $k = 0.01$. Solid-wall boundary conditions are used along $x = 0$ and $y = 0$. Outflow boundary conditions are used along $x = 50$ and $y = 50$. Figure 5a shows the velocity fields and Fig. 5b shows profiles of the pressure p, temperature T, and 100 times the mass fraction of the first species, $100z_1$ (here we show $100z_1$, not z_1 itself, for better visualization) on the line $y = x (x \geq 0.0)$ by the random projection method (4.7) at times $t = 1, 2, 4$, and 6.

It can be seen that the detonation front remains circular and no spurious nonphysical wave is generated when using the random projection method (4.7). On the other hand, if one uses the deterministic method, the detonation front does not remain circular and a spurious nonphysical wave is generated if the same grid size and time step are used.

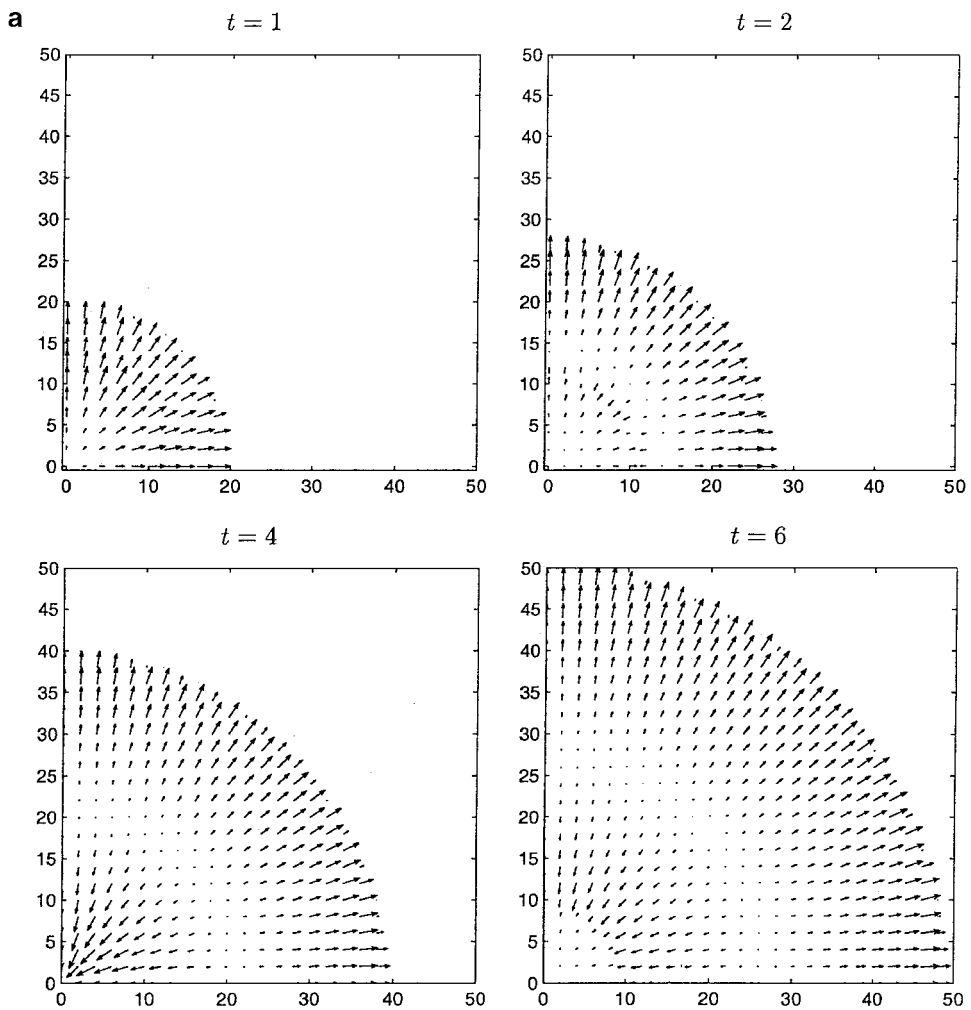

FIG. 5. Numerical solutions of Example 5.5 calculated by the 2D random projection method (4.7) with $h = 0.5$, $k = 0.01$. (a) Velocity fields at different times. (b) Profiles of pressure p (−−), temperature T (−), and the mass fraction of the first species multiplied by 100, $100z_1$ (–·), on the line $y = x$ $(x \geq 0.0)$ at different times.

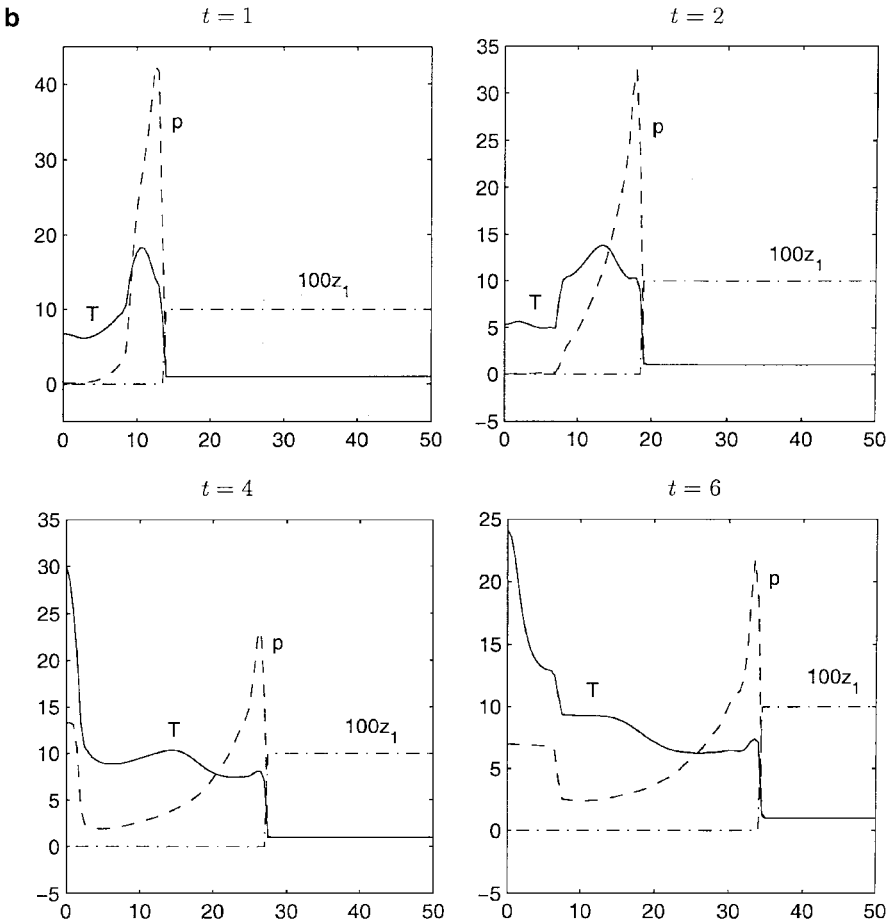

FIG. 5—*Continued*

EXAMPLE 5.6. This is a two-dimensional example analogous to Example 5.4, i.e., the parameters $M, N, \gamma, T_1, T_2, B_1, B_2, \alpha_1, \alpha_2, q_1, \ldots, \nu''_{5,2}$ are the same as those in Example 5.4. The initial data are given by

$$(\rho, u, v, p, z_1, z_2, z_3, z_4, z_5)(x, y, 0) = \begin{cases} (\rho_l, u_l, v_l, p_l, (z_1)_l, (z_2)_l, (z_3)_l, (z_4)_l, (z_5)_l), & \text{if } x \le \xi(y), \\ (\rho_r, u_r, v_r, p_r, (z_1)_r, (z_2)_r, (z_3)_r (z_4)_r, (z_5)_r), & \text{if } x > \xi(y), \end{cases}$$

where

$$\xi(y) = \begin{cases} 12.5 - |y - 12.5|, & |y - 12.5| \le 7.5, \\ 5, & |y - 12.5| > 7.5, \end{cases}$$

with $p_l = 40.0$, $\rho_l = 2.0$, $u_l = 10.0$, $v_l = 0.0$, $(z_1)_l = 0.0$, $(z_2)_l = 0.0$, $(z_3)_l = 0.17$, $(z_4)_l = 0.63$, and $(z_5)_l = 0.2$, and with $p_r = 1.0$, $\rho_r = 1.0$, $u_r = 0.0$, $v_r = 0.0$, $(z_1)_r = 0.08$, $(z_2)_r = 0.72$, $(z_3)_r = 0.0$, $(z_4)_r = 0.0$, and $(z_5)_r = 0.2$.

This problem is solved on the domain $[0, 150] \times [0, 25]$ with $h = 0.5$ and $k = 0.01$. Solid-wall boundary conditions are used along $y = 0$ and $y = 25$. Inflow boundary

conditions are used along $x = 0$ and outflow boundary conditions are used along $x = 150$. One important feature of this solution is that the triple points along the detonation front travel in the transverse direction and bounce back and forth against the upper and lower walls, forming a cellular pattern. Behind the detonation front, there is a very strong shock. Figure 6a shows density contours calculated by the random projection method (4.7) at several different times. Figure 6b shows profiles of pressure p, temerature T, and 300 times the mass fraction of the first species, $300z_1$, on the line $y = 12.5$ at times $t = 2, 4, 6$, and 8.

One can see that no spurious nonphysical wave is generated when the random projection method is used (4.7). However, if one uses the deterministic method, a spurious nonphysical wave is generated if the same grid size and time step are used.

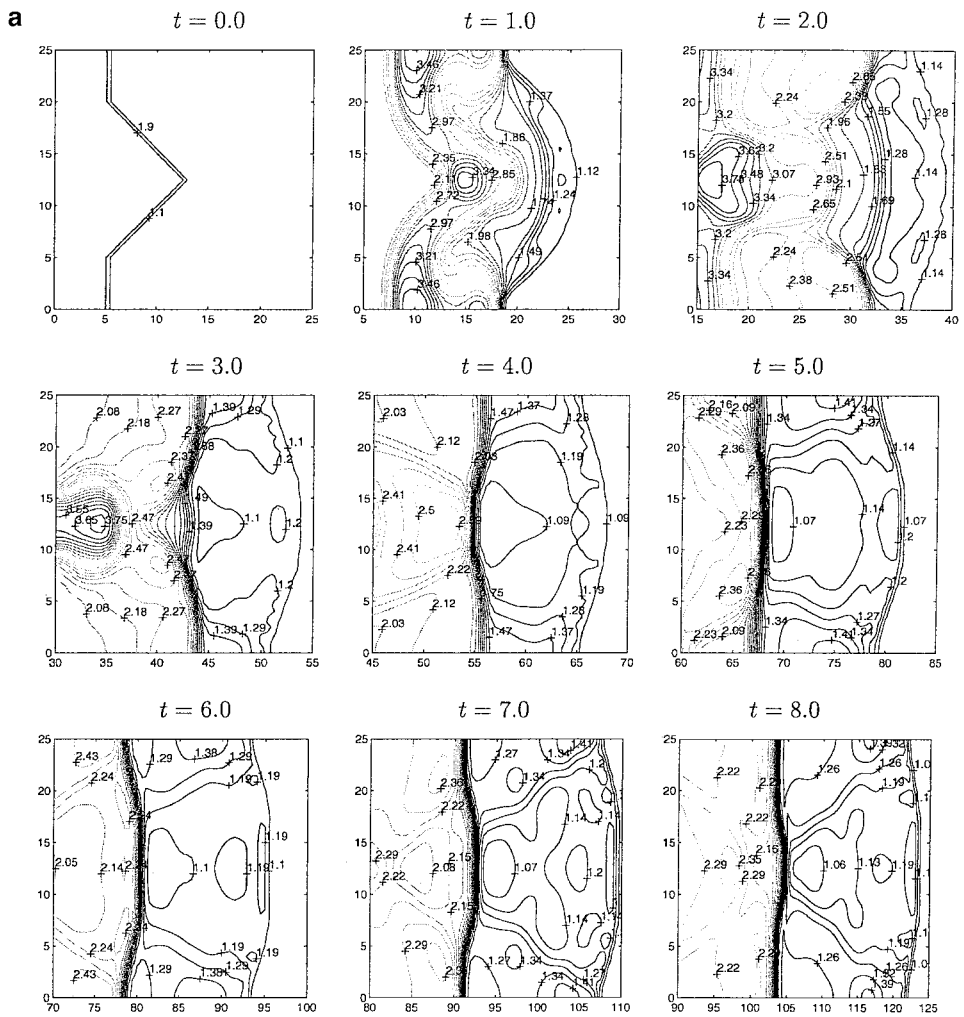

FIG. 6. Numerical solutions of Example 5.6 calculated by the 2D random projection method (4.7) with $h = 0.5$, $k = 0.01$. (a) Density contours at different times. (b) Profiles of pressure p (−−), temperature T (−), and the mass fraction of the first species multiplied by 300, $300z_1$ (–·), on the line $y = 12.5$ at different times.

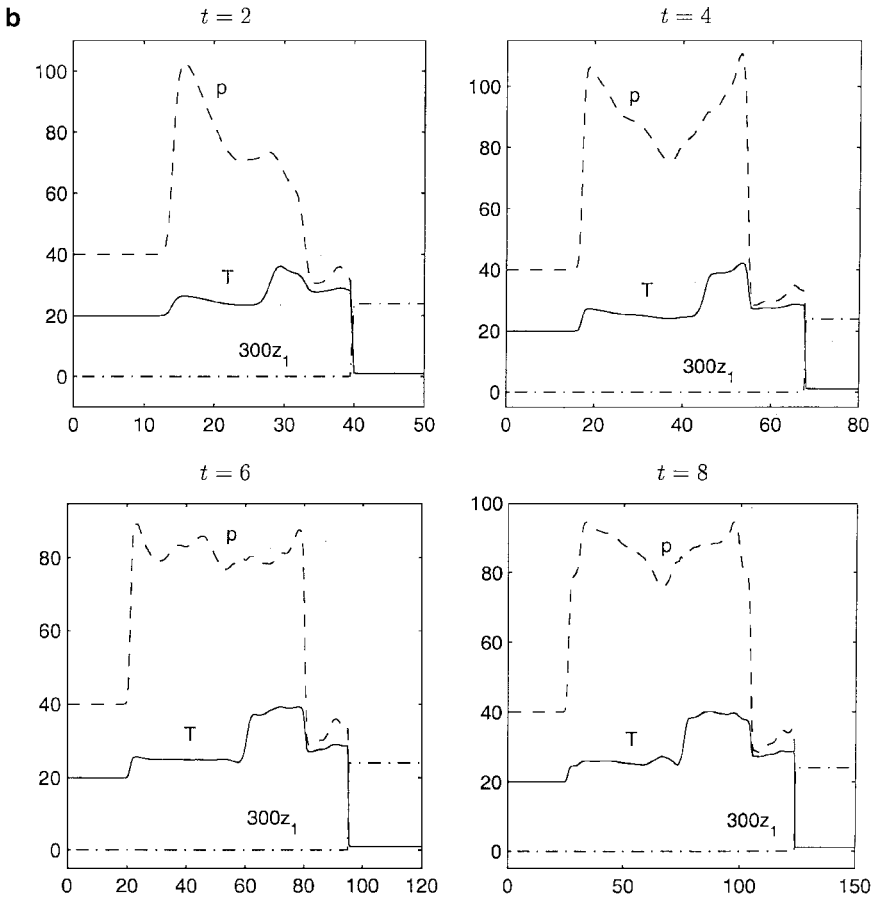

FIG. 6—*Continued*

6. CONCLUSIONS

In this paper we extend the random projection method to underresolved computation of stiff multispecies detonations. This method is based on the random projection method proposed by the authors for general hyperbolic systems with stiff reaction terms [1]. The key idea of this method is to randomize the ignition temperatures in a suitable domain. Numerical experiments in both one- and two-dimensional problems demonstrate that this method, although very simple and efficient, provides physically correct solutions with a high resolution when the small chemical scale is not numerically resolved.

ACKNOWLEDGMENTS

W. Bao thanks the School of Mathematics of the Georgia Institute of Technology and the Department of Mathematics of the University of Wisconsin-Madison for their hospitality during his extended visits there.

REFERENCES

1. W. Bao and S. Jin, The random projection method for hyperbolic conservation laws with stiff reaction terms, *J. Comput. Phys.* **163**, 216 (2000).

2. W. Bao and S. Jin, The random projection method for stiff detonation waves, *SIAM J. Sci. Comp.* **23**, 1000 (2001).
3. A. C. Berkenbosch, E. F. Kaasschieter, and R. Klein, Detonation capturing for stiff combustion chemistry, *Combust. Theory Modeling* **2**, 313 (1998).
4. M. Ben-Artzi, The generalized Riemann problem for reactive flows, *J. Comput Phys.* **81**, 70 (1989).
5. A. Bourlioux, A. Majda, and C. Roytburd, Theoretical and numerical structure for unstable one-dimensional detonations, *SIAM J. Appl. Math.* **51**, 303 (1991).
6. T. R. A. Bussing and E. M. Murman, Finite-volume method for the calculation of compressible chemically reacting flows, *AIAA J.* **26**, 1070 (1987).
7. I.-L. Chern, J. Glimm, O. McBryan, B. Plohr, B. Yaniv, and S. Yaniv, Front tracking for gas dynamics, *J. Comput. Phys.* **62**, 83 (1986).
8. A. J. Chorin, Random choice methods with applications to reacting gas flow, *J. Comput. Phys.* **25**, 253 (1977).
9. P. Colella, Glimm's method for gas dynamics, *SIAM J. Sci. Stat. Comput.* **3**, 76 (1982).
10. P. Colella, A. Majda, and V. Roytburd, Theoretical and numerical structure for reacting shock waves, *SIAM J. Sci. Stat. Comput.* **7**, 1059 (1986).
11. B. Engquist and B. Sjogreen, *Robust difference approximations of stiff inviscid detonation Waves*, CAM Report 91-03 (UCLA, 1991).
12. R. Fedkiw, T. Aslam, and S. Xu, The ghost fluid method for deflagration and detonation discontinuities, *J. Comput. Phys.* **154**, 393 (1999).
13. P. Gerlinger, P. Stoll, and D. Brüggemann, An implicit multigrid method for the simulation of chemically reacting flows, *J. Comput. Phys.* **146**, 322 (1998).
14. I. Glassman, *Combustion* (Academic Press, San Diego, 1987).
15. J. Glimm, Solutions in the large for nonlinear hyperbolic systems of equations, *Commun. Pure Appl. Math.* **18**, 697 (1965).
16. D. F. Griffiths, A. M. Stuart, and H. C. Yee, Numerical wave propagation in an advection equation with a nonlinear source term, *SIAM J. Numer. Anal.* **29**, 1244 (1992).
17. J. M. Hammersley and D. C. Handscomb, *Monte Carlo Methods* (Methuen, London, 1965).
18. C. Helzel, R. J. LeVeque, and G. Warnecke, A modified fractional step method for the accurate approximation of detonation waves, submitted for publication.
19. S. Jin and Z. P. Xin, The relaxation schemes for systems of conservation laws in arbitrary space dimensions, *Commun. Pure Appl. Math.* **48**, 235 (1995).
20. R. J. LeVeque and H. C. Yee, A study of numerical methods for hyperbolic conservation laws with stiff source terms, *J. Comput. Phys.* **86**, 187 (1990).
21. H. N. Najm, P. S. Wyckoff, and O. M. Knio, A semi-implicit numerical scheme for reacting flow, *J. Comput. Phys.* **143**, 381 (1998).
22. S. Osher and R. P. Fedkiw, Level set methods: An overview and some recent results, *J. Comput. Phys.* **169**, 463 (2001).
23. R. B. Pember, Numerical methods for hyperbolic conservation laws with stiff relaxation. I. Spurious solutions, *SIAM J. Appl. Math.* **53**, 1293 (1993).
24. V. Smiljanoyski and R. Klein, Flame front tracking via in cell reconstruction, in *Proceedings, 5th International Conference on Hyperbolic Problems, Theory, Numerics, and Applications* (World Scientific Press, 1996), pp. 456–463.
25. M. A. Sussman, *Source Term Evaluation for Combustion Modeling*, AIAA paper 93-0239 (1993).
26. F. A. Williams, *Combustion Theory* (Addison–Wesley, Reading, MA, 1985).
27. G. J. Wilson and M. A. Sussman, Computation of unsteady shock-induced combustion using logarithmic species conservation equations, *AIAA J.* **31**, 294 (1993).
28. H. C. Yee and J. L. Shinn, Semi-implicit and fully implicit shock-capturing methods for nonequilibrium flows, *AIAA J.* **27**, 299 (1989).